Cooperative Hybridization of Oligonucleotides

Supplementary Information

David Yu Zhang[1]

[1] *California Institute of Technology, Pasadena, CA 91125*

present address: Wyss Institute, Harvard University, Boston, MA 02115

S1. DNA sequence design

The lengths and sequences of the 2 and 3 domains were chosen so that spontaneous dissociation of $P1$ from state I or J would be extremely unlikely. For average 15-mers (with $\Delta G^0 \approx 21$ kcal/mol), the dissociation time is estimated to be roughly 10 years, which is far longer than the timescale of the reactions being monitored. However, in order to account for synthesis errors that could destabilize the binding of these domains to their complements, the lengths of the 2 and 3 domains were chosen to be 18 nt. It is expected that the devices would work similarly for domains 2 and 3 of equal or longer length, except insofar as the kinetics of branch migration would be slowed for long domains.

There are two criteria on the lengths and sequences of the 1 and 4 domains:

First, the thermodynamics of 1 and 4 binding to their complement domains in $D1$ should overcome the configuration entropy loss of colocalizing another molecule ($T1 + T2 + D1 \rightarrow P1 + H1$). Consider the equilibrium distribution of $T1$, $T2$, $D1$, $P1$, and $H1$:

$$\begin{aligned} K_{\text{eq}} &= \frac{[P1][H1]}{[T1][T2][D1]} = e^{-\Delta \text{G}^\circ/RT} \\ \frac{[P1][H1]}{[T1][T2]} &= e^{-\Delta \text{G}^\circ/RT \,+\, \ln([D1])} \\ &= e^{-(\Delta \text{G}^\circ - RT\ln([D1]))/RT} \end{aligned}$$

The reaction is driven to more than 50% completion when $\frac{[P1][H1]}{[T1][T2]} > 1$, which is equivalent to saying $\Delta \text{G}^\circ - RT\ln([D1]) < 0$. The value of ΔG° for the reaction can be calculated as:

$$\begin{aligned} \Delta \text{G}^\circ &= \Delta \text{G}^\circ(P1) + \Delta \text{G}^\circ(H1) - \Delta \text{G}^\circ(T1) - \Delta \text{G}^\circ(T2) - \Delta \text{G}^\circ(D1) \\ &= \Delta \text{G}^\circ(H1) - \Delta \text{G}^\circ(D1) \\ &= (\Delta \text{G}^\circ(1) + \Delta \text{G}^\circ(2) + \Delta \text{G}^\circ(3) + \Delta \text{G}^\circ(4) - 2 \cdot \Delta \text{G}^\circ_{init}) - (\Delta \text{G}^\circ(2) + \Delta \text{G}^\circ(3) - \Delta \text{G}^\circ_{init}) \\ &= \Delta \text{G}^\circ(1) + \Delta \text{G}^\circ(4) - \Delta \text{G}^\circ_{init} \end{aligned}$$

where $\Delta G^\circ(1)$ denotes the hybridization energy of domain 1 to its complement 1^*, and ΔG_{init} denotes the entropy penalty of initiating a helix formation [1]. The standard free energies of $T1$, $T2$, and $P1$ are 0, since they have been designed not to possess secondary structure.

The concentration of $D1$ is typically higher than that of $T1$ and $T2$, and does not change significantly through the course of the reaction, so $[D1]$ can be approximated as $[D1]_0$, the initial concentration of $D1$. Substituting the expansion of ΔG° into the inequality $\Delta G^\circ - RT\ln([D1]) < 0$,

$$\Delta G^\circ(1) + \Delta G^\circ(4) - \Delta G^\circ_{init} - RT\ln([D1]) < 0$$
$$\Delta G^\circ(1) + \Delta G^\circ(4) < \Delta G^\circ_{init} + RT\ln([D1])$$

ΔG°_{init} is approximated to be -1.8 kcal / mol at 25 °C [1], and at $[D1]$ = 10 nM, $-RT\ln([D1]) = -10.9$ kcal/mol. Thus, $\Delta G^\circ(1) + \Delta G^\circ(4) < -12.7$ kcal / mol. Assuming $\Delta G^\circ(1) \approx \Delta G^\circ(4)$, $\Delta G^\circ(1) < -6.4$ kcal/mol. This value roughly corresponds to lower bound of approximately 5 nt for domains with roughly equal distribution of G/C and A/T bases.

Second, the thermodynamics of 1 and 4 binding to their complement domains in $D1$ should be weak enough so that if only one target is present, then that target is thermodynamically favored to be not bound to $D1$. Similar analysis to the above leads to the upper bounds: $\Delta G^\circ(1), \Delta G^\circ(4) \geq RT\ln(c) + \Delta G^\circ_{init} = -12.7$ kcal / mol, corresponding to roughly 10 nt for domains with roughly equal distribution of G/C and A/T bases. Consequently, the lengths of both the 1 and 4 domains were chosen to be 8 nt.

The domain sequences used in this paper were designed to be minimally interacting. Special emphasis was placed on ensuring that single-stranded targets and products ($T1$, $T2$, $P1$, $T4$) possessed no significant secondary structure. Although it is expected that the designs will function qualitatively similarly for strands with secondary structure, secondary structure is known to slow down the kinetics of hybridization and branch migration processes [2].

S2. Matlab code for simulating reactions and fitting rate constants

The Matlab script for fitting the k_1 rate constant (using the data shown in Fig. S1B) is shown below:

```
k1 = log(1E6);
s1 = log(4e13);
[k, fval] = fminunc(@rate1, [k1, s0]);
exp(k(1)) %output rate constant
exp(k(2)) %output scaling constant
```

The fminunc function minimizes the parameters for the rate constant k_1 and the scaling constant s_1 for the function "rate1" shown below:

```
function err_func = rate1(input)
data = load('/Users/daveyzhang/Desktop/work/expt/Fluorescence/20090119/003m.txt');
k = exp(input(1));
scalingconst = exp(input(2));
err_func = 0;
options = odeset('RelTol', 1e-4, 'AbsTol', 1e-30);
datasize = size(data, 1);

%0.2 nM data
t = data(6:datasize,1)-300;
y0 = [1e-9, 2e-10, 0, 3e-9, 0];
[t, y2] = ode23s(@rdy, t, [k, y0], options);
ye = y2(:,6) * scalingconst;
for i = 7:size(data, 1)
    err_func = err_func + (ye(i-6) - (data(i,3)-data(5,3)+data(5,2)-data(i,2)))^2;
end

%0.4 nM data
t = data(6:datasize,1)-300;
y0 = [1e-9, 4e-10, 0, 3e-9, 0];
[t, y4] = ode23s(@rdy, t, [k, y0], options);
ye = y4(:,6) * scalingconst;
for i = 7:size(data, 1)
    err_func = err_func + (ye(i-6) - (data(i,4)-data(5,4)+data(5,2)-data(i,2)))^2;
end

%0.6 nM data
t = data(6:datasize,1)-300;
y0 = [1e-9, 6e-10, 0, 3e-9, 0];
[t, y6] = ode23s(@rdy, t, [k, y0], options);
ye = y6(:,6) * scalingconst;
for i = 7:size(data, 1)
    err_func = err_func + (ye(i-6) - (data(i,5)-data(5,5)+data(5,2)-data(i,2)))^2;
end
```

This "rate1" function in turn calls upon the following "rdy" function that defines the ordinary differential equations:

```
function dy = rdy(t, y)
%J + In1 -> P1
%P1 + R -> F
krep = 1.3e7; %fitted earlier
k = y(1);
```

```
dy = zeros(6,1);
dy(2) = - k * y(2) * y(3);
dy(3) = - k * y(2) * y(3);
dy(4) = k * y(2) * y(3) - krep * y(4) * y(5);
dy(5) = -krep * y(4) * y(5);
dy(6) = krep * y(4) * y(5);
```

Similar code was used to fit other rate constants.

S3. Characterization of individual rate constants

The individual rate constants of various intermediate reactions are characterized. The k_{rep} rate constant for the $P1 + R \rightarrow F + Fw$ reporter reaction is measured in Fig. S1A to be $1.3 \pm 0.5 \cdot 10^7$ M^{-1} s^{-1}. This rate constant is significantly higher than those of similar reporter complexes [3, 4], though the reason for this is not understood. The rate constants of strand displacement reactions involving fluorophore and quencher-labelled DNA oligonucleotides generally cannot be predicted as reliably as those of unfunctionalized DNA [4, 5].

Th k_{f1} and k_{f2} rate constants are measured in Fig. S2B and S2C, respectively, to be $2.1 \pm 0.7 \cdot 10^6$ M^{-1} s^{-1} and $1.4 \pm 0.2 \cdot 10^6$ M^{-1} s^{-1}. These values are consistent with previous characterizations of strand displacement rate constants, which ranged from $3 \cdot 10^5$ M^{-1} s^{-1} to $6 \cdot 10^6$ M^{-1} s^{-1} for 8 nt toeholds, depending on the sequence of the toehold [4].

S4. Concentration quantitation from Fig. 2.

The cooperative and simultaneous nature of the hybridization of two target oligonucleotides to the two-stranded complex means that the cooperative hybridization mechanism can easily be applied to quantitating nucleic acids. For example, in Fig. 2, consider $T4$ as a standard of known concentration, against which we measure the concentration/quantity of a sample with an unknown amount of target oligonucleotide $T3$.

With increased amounts of $T3$ in the sample solution, the equilibrium fluorescence of the mixture of $T3$ and $T4$ decreases, until the minimum where the quantity of $T3$ exceeds that of $T4$. Thus, one can use cooperative hybridization to accurately determine the concentration of a nucleic acid species, relative to that of a standard oligonucleotide of independent sequence.

The equilibrium fluorescence of the mixture of $T3$ and $T4$ initially decreases linearly with the concentration of $T3$; thus linear response facilitates the quantitation process. To mathematically show that the fluorescence is linear in the quantity of $T3$, we first consider the components of the observed fluorescence.

There are three sources of fluorescence signal in the experiments described in Fig. 2: the unquenched fluorophores in $T4$, the quenched fluorophores in $J2$ and $H2$, and the background fluorescence. Define b to

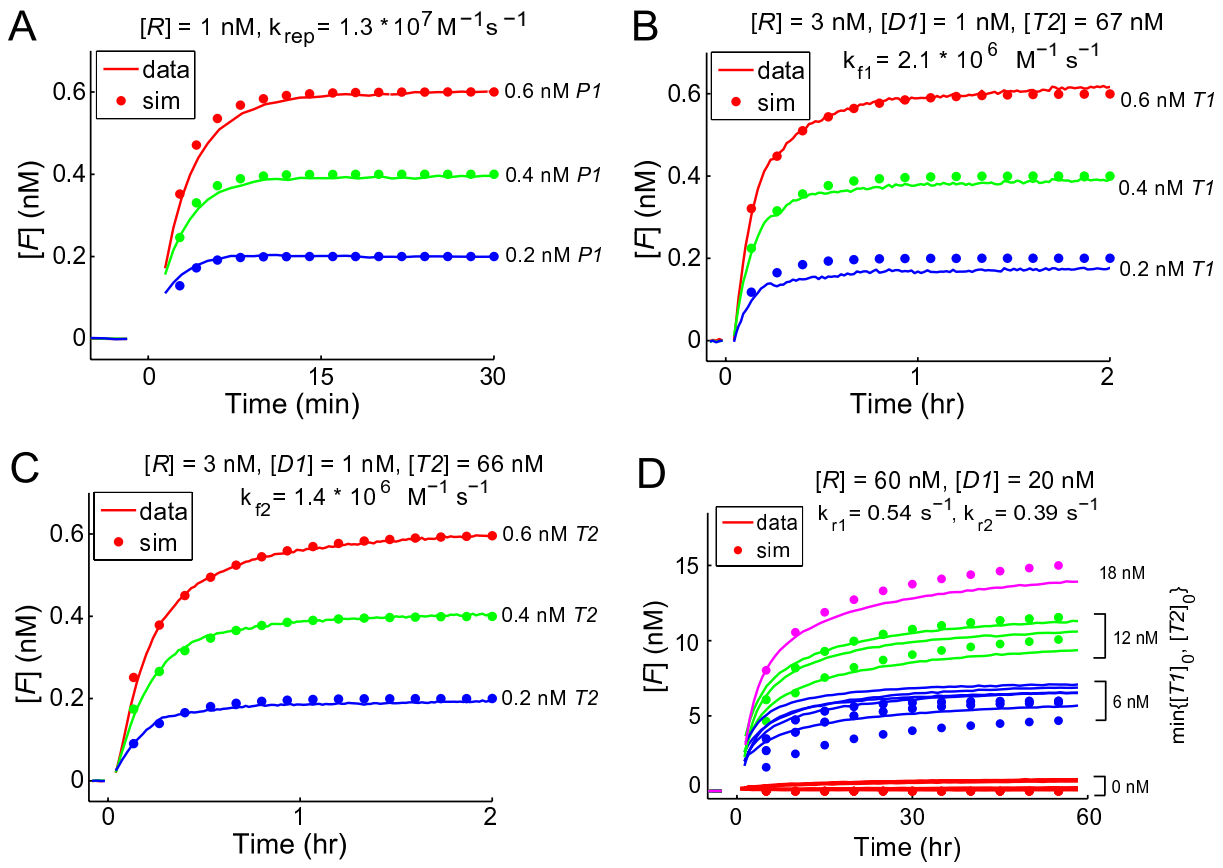

FIG. S1: Rate constant characterization. **(A)** Reporter R was present in the cuvette initially, and various amounts of $P1$ were added at $t \approx 0$. The dotted lines show the simulations of the reaction given the listed concentrations and the fitted rate constant $k_{rep} = 1.3 \cdot 10^7$ M^{-1} s^{-1}. **(B)** The rate constant k_{f1} was fitted by observing the kinetics of the $J + T1 \rightarrow P1 + H1$ reaction, using the fitted k_{rep} from panel (A). Prior to the start of the reaction, $D1$ and a large excess of $T2$ were mixed and allowed to equilibrate for over 1 hour. $T2$ was added at $t \approx 0$. **(C)** The rate constant k_{f2} was similar fitted by pre-reacting $D1$ and $T1$ to form I, which then started reacting with $T2$ when the latter was introduced at $t \approx 0$. **(D)** The rate constants k_{r1} and k_{r2} were fitted simultaneously using the results of the full system shown in Fig. 2. Simulations of the reactions in panels (B) and (C) including the reverse reactions $J \rightarrow D1 + T2$ and $I \rightarrow D1 + T1$ yielded quantitatively similar results and did not change the best fit range constants (to 2 significant digits). Note that several simulation traces show near identical kinetics and cannot be visually distinguished in the plot.

be the background fluorescence. Define a to be the fluorescence per unit of the unquenched fluorophore. Define q to be the quenching ratio of the fluorophore (the fluorescence of the unquenched fluorophore divided by the fluorescence of the quenched fluorophore). Thus, the fluorescence f of a solution can be written as:

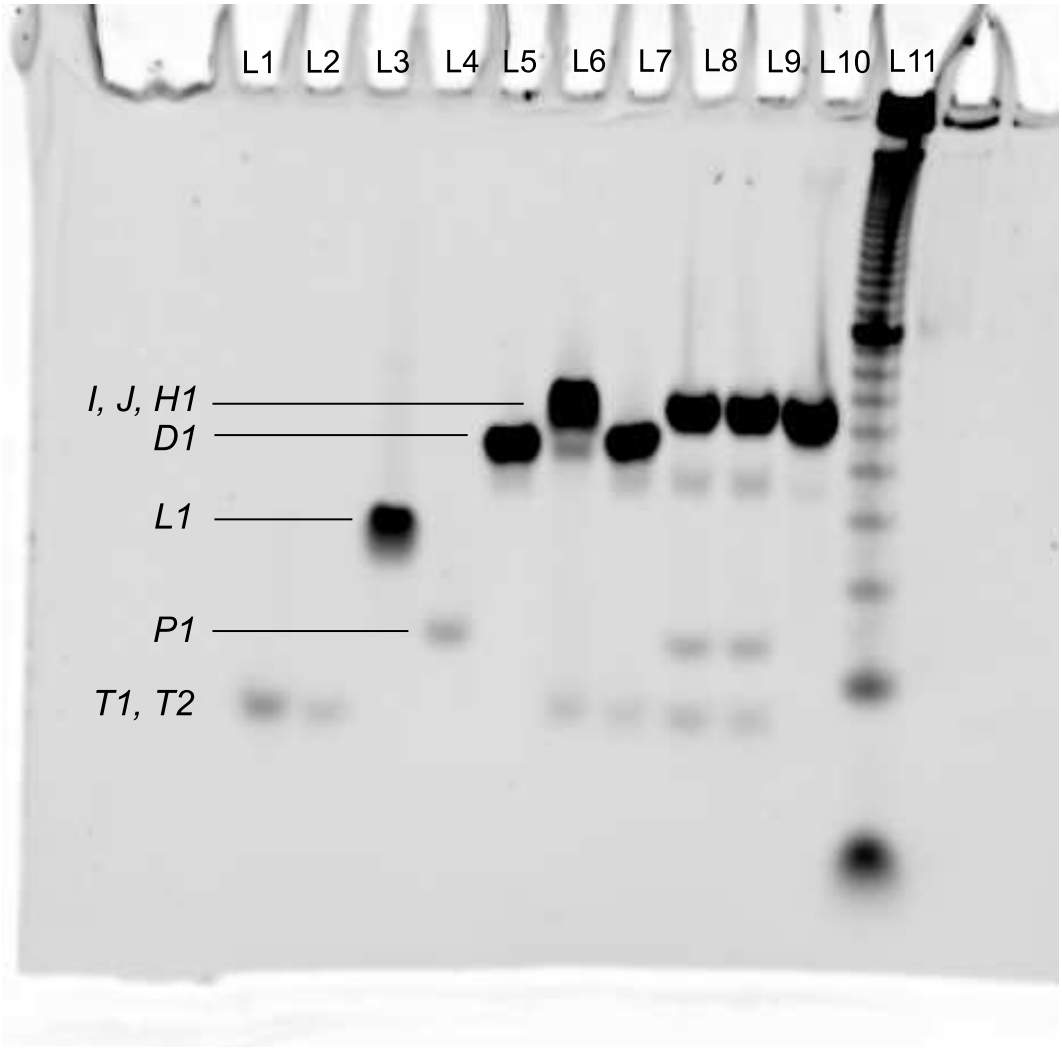

FIG. S2: Native polyacrylamide gel electrophoresis (PAGE) on cooperative strand displacement. This experiment used 12% acrylamide (19:1 acrylamide:bis), diluted from 40% acrylamide stock (Ambion). Native loading dye containing xylene cyanol-FF (XCFF) in 50% glycerol was added to all samples, achieving final glycerol concentration of 10% by volume. Gels were run at 25 °C using a Novex chamber with external temperature bath. Gels were stained with Sybr-Gold stain (Invitrogen), and scanned with a Bio-Rad Molecular Imager. "30 min" denotes that the strands and complexes were mixed and allowed to react at 25 °C for 30 minutes. $L1$ is the bottom strand of $D1$ ($L1$ and $P1$ together comprise $D1$). $T1$, $T2$, and $P1$ stains less efficiently than other strands and complexes due to their short lengths and single-stranded nature. The single-stranded $P1$ band appears only when both $T1$ and $T2$ are present. Intermediate I migrates at approximately the same speed as $H1$. Intermediate J is assumed to dissociate on the time scale of running the gel.

Lane	Contents	Lane	Contents
1	$T1$ (200 nM)	7	$D1$ (200 nM) + $T2$ (400 nM) [30 min]
2	$T2$ (200 nM)	8	$D1$ (200 nM) + $T1$ (400 nM) + $T2$ (400 nM) [30 min]
3	$L1$ (200 nM)	9	$D1$ (200 nM) + $T1$ (400 nM) + $T2$ (400 nM) [annealed]
4	$P1$ (200 nM)	10	$H1$ (200 nM) [annealed]
5	$D1$ (200 nM)	11	10 nt duplex ladder
6	$D1$ (200 nM) + $T1$ (400 nM) [30 min]		

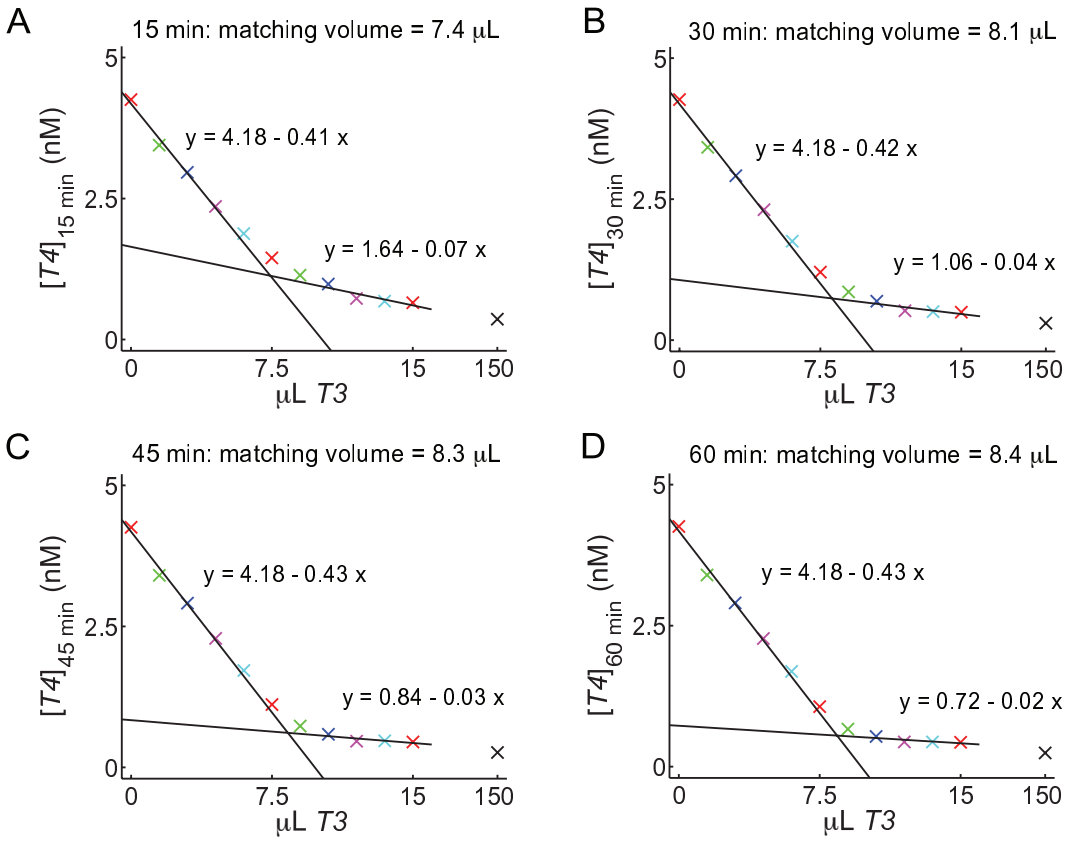

FIG. S3: Concentration inference from the data in Fig. 2B. The fluorescence levels of the various traces at 15 min, 30 min, 45 min, and 60 min are plotted in **(A)**, **(B)**, **(C)**, and **(D)**, respectively. Each sub-figure shows two linear fits, one to the first 4 data points and one to the last 4 data points (other than the 150 μL). The intersection of the two linear fits is the inferred matching volume of $T3$, the volume of $T3$ in which the quantity of $T3$ and $T4$ are stoichiometrically balanced.

$$\begin{aligned} f &= a[T4] + \frac{a}{q}([J2] + [H2]) + b \\ &= \frac{a(q-1)}{q}[T4] + \frac{a[T4]_{\text{tot}}}{q} + b \end{aligned}$$

where $[T4]_{\text{tot}} = [T4] + [J2] + [H2]$ is the total concentration of $T4$ in solution. As can be seen, the fluorescence f is linear in $[T4]$.

Idealized case.

In the idealized case of when the sample solution containing the target reaches equilibrium with the test solution containing the standard and device, and where the fluorescence readout is infinitely accurate, the concentration of the target in the sample solution can be easily calculated from a single experiment.

Define x to be the volume of sample solution that reacted with y volume of test solution. The system

operates under the assumption that $y \geq x$. Define the concentration of $T3$ in the sample solution to have been $[T3]_s$. Define the total concentrations of $T4$ and $D2$ (including the portion sequestered in $L2$) in the test solution to have been $[T4]_t$ and $[D2]_t$, respectively. Thus, there are $x[T3]_s$ moles of $T3$, $y[T4]_t$ moles of $T4$, and $y[D2]_t$ moles of $D2$. In order for quantitation to be possible, $y[T4]_t > x[T3]_s$ (i.e. standard exceeds target).

Define $[T4]_m$, $[D2]_m$, and $[J2]_m$ to be the concentrations of free $T4$, free $D2$, and intermediate $J2$ in the mixture of the sample and test solutions at equilibrium. $[T4]_m$ is inferred from the fluorescence level, and we wish to derive $[T3]_s$, the concentration of the target in the initial sample solution.

$$\begin{aligned} \frac{y[T4]_t - x[T3]_s}{x+y} &= [T4]_m + [J2]_m \\ \frac{y[D2]_t - x[T3]_s}{x+y} &= [D2]_m + [J2]_m \end{aligned}$$

Reorganizing,

$$\begin{aligned} [J2]_m &= \frac{y[T4]_t - x[T3]_s}{x+y} - [T4]_m \\ [D2]_m &= [T4]_m + \frac{y([D2]_t - [T4]_t)}{x+y} \end{aligned}$$

From the equilibrium of the mixture:

$$\begin{aligned} K_{eq} &= \frac{[J2]_m}{[T4]_m[D2]_m} \\ &= \frac{\frac{y[T4]_t - x[T3]_s}{x+y} - [T4]_m}{[T4]_m([T4]_m + \frac{y([D2]_t - [T4]_t)}{x+y})} \end{aligned}$$

$$K_{eq}[T4]_m([T4]_m + \frac{y([D2]_t - [T4]_t)}{x+y}) + [T4]_m = \frac{y[T4]_t - x[T3]_s}{x+y}$$

$$[T3]_s = \frac{y[T4]_t}{x} - \frac{K_{eq}y([D2]_t - [T4]_t) + x + y}{x}[T4]_m - \frac{K_{eq}(x+y)}{x}[T4]_m^2 \quad (1)$$

Every variable on the right hand side of the equation is known (with K_{eq} calculated from the ΔG° of the reaction); thus, $[T3]_s$ can be calculated from observed fluorescence.

Quantitation using a calibration series.

Given that at experimental concentrations, the reactions could take quite long to reach equilibrium, it is possible instead to use a series of experiments with various different volumes of the sample solution reacting with the test solution. This is the method used to quantitate the concentration of $T3$ shown in Fig. 2BC. As the volume of the sample solution increases, the amount of $T3$ eventually overtakes that of the standard $T4$. The volume of sample solution at which the amount of $T3$ stoichiometrically matches that of $T4$ is here denoted as the *matching volume*.

When the matching volume of the sample solution is added to the test solution, then at equilibrium all of the $T4$ will be sequestered in waste $H2$ and quenched. Further addition of sample solution will only slightly decrease the fluorescence (due to dilution of the quenched fluorophore in $H2$). It takes a long time for equilibrium to be established when the exact matching volume of the sample solution is added due to the second-order nature of the $J2 + T3 \rightarrow P2 + H2$ reaction, but equilibrium is more quickly approached when the amount of sample solution added deviates significantly from the matching volume (the reaction kinetics become pseudo-first order due to the excess of either $J2$ or $T3$).

Given the fluorescence of various mixtures with different amounts of sample solution at a particular time point, the matching volume can be estimated by the intersection of two linear fits of fluorescence to sample solution volume (Fig.S2). See the following section "Pseudo-linearity" for the justification on why fluorescence is expected to linearly decrease with the amount of $T3$ added. The data from the later time points are expected to be more reliable because the reaction has proceeded closer to equilibrium, and because the earlier data points may be affected more strongly by incomplete mixing and experimental error on the reported time points. The linear fits in Fig. S2 use 4 data points each; Table S2 show the inferred matching volumes based on linear fits using 3, 4, and 5 data points. As can be seen, the inferred matching volumes are quite similar regardless of how many data points are used in the linear fits.

From the data shown, the matching volume is seen to be 8.4 ± 1.0 μL. Assuming that the concentration of the standard $T4$ is accurate at 5 nM, the total amount of $T4$ is 5 nM $\cdot$1.5 mL= 7.5 pmol, and the inferred concentration of $T3$ in the sample solution is is $\frac{7.5\text{pmol}}{8.4 \pm 1.0 \mu\text{L}} = 0.89 \pm 0.12$ μM, or 0.9 ± 0.1 μM after accounting for significant digits.

	3 points	4 points	5 points
15 min	7.8 μL	7.4 μL	7.5 μL
30 min	8.1 μL	8.1 μL	8.1 μL
45 min	8.3 μL	8.3 μL	8.3 μL
60 min	8.3 μL	8.4 μL	8.4 μL

Table S2: Inferred matching volume of $T3$ from data in Fig. 2B.

Pseudo-linearity.

We wish to show that the fluorescence ($[T4]_m$) decreases pseudo-linearly with the amount of $T3$ added ($x[T3]_s$). Rearranging eq. (5),

$$K_{eq}(x+y)[T4]_m^2 + (K_{eq}y([D2]_t - [T4]_t) + x + y)[T4]_m - (y[T4]_t - x[T3]_s) = 0$$

Solving this quadratic relation,

$$\begin{aligned}[T4]_m &= -\frac{K_{eq}y([D2]_t - [T4]_t) + x + y}{2K_{eq}(x+y)} \\ &\quad + \frac{\sqrt{(K_{eq}y([D2]_t - [T4]_t) + x + y)^2 + 4K_{eq}(x+y)(y[T4]_t - x[T3]_s)}}{2K_{eq}(x+y)}\end{aligned}$$

The second term can be approximated as

$$\frac{1}{2K_{eq}(x+y)}(x + y + K_{eq}y([D2]_t - [T4]_t) + 2K_{eq}(y[T4]_t - x[T3]_s))$$

if $2K_{eq}(y[T4]_t - x[T3]_s)$ is small compared to $x + y + K_{eq}y([D2]_t - [T4]_t)$. We will show that this is the case shortly. For now, we continue using the approximation, substituting back into the expression for $[T4]_m$:

$$\begin{aligned}[T4]_m &\approx -\frac{K_{eq}y([D2]_t - [T4]_t) + x + y}{2K_{eq}(x+y)} + \frac{x + y + K_{eq}y([D2]_t - [T4]_t) + 2K_{eq}(y[T4]_t - x[T3]_s)}{2K_{eq}(x+y)} \\ &= \frac{2K_{eq}(y[T4]_t - x[T3]_s)}{2K_{eq}(x+y)} \\ &= \frac{y[T4]_t}{x+y} - \frac{1}{x+y}x[T3]_s\end{aligned}$$

The final relationship between $[T4]_m$ and $x[T3]_s$ is thus seen to be approximately linear.

This pseudo-linearity depends upon the condition:

$$2K_{eq}(y[T4]_t - x[T3]_s) \ll x + y + K_{eq}y([D2]_t - [T4]_t)$$

For our purpose, let us solve for the conditions under which:

$$2K_{eq}(y[T4]_t - x[T3]_s) < 0.5(x + y + K_{eq}y([D2]_t - [T4]_t))$$

When this is true, the difference between the approximate $[T4]_m$ and the real $[T4]_m$ is less than 20%. Rearranging this relation,

$$4K_{eq}(y[T4]_t - x[T3]_s) \;<\; x + y + K_{eq}y([D2]_t - [T4]_t)$$

The left hand side is smaller than $4K_{eq}y[T4]_t$, and the right hand side is greater than y, so a sufficient condition is:

$$\begin{aligned} 4K_{eq}y[T4]_t &< y \\ K_{eq} &< \frac{1}{4[T4]_t} \end{aligned}$$

Recall that $K_{eq} = \frac{[J2]}{[T4][D2]}$.

$$\begin{aligned} \frac{[J2]}{[T4][D2]} &< \frac{1}{4[T4]_t} \\ \frac{[J2]}{[T4]} &< \frac{[D2]}{4[T4]_t} \end{aligned}$$

When $[D2]_t \geq 2[T4]_t$, $[D2]$ is necessarily greater than $[T4]_t$, so the right hand side is greater than $\frac{1}{4}$. Thus, the necessary condition for the approximation is satisfied whenever $\frac{[J2]}{[T4]} < \frac{1}{4}$. This equates to saying that operational concentrations must be low enough that the $T4 + D2 \rightleftharpoons J2$ reaction favors the reactants by at least a 4:1 ratio.

S5. Alternate mechanism for digitally comparing nucleic acid concentrations

Fig. 4 in the main paper shows methods for performing thresholded amplified detection of an oligonucleotide target. Because the goal of those designs were not only to provide a sigmoidal threshold, but also to provide amplification to improve sensitivity, the digital nature of the response was somewhat compromised. Here, an alternative mechanism for implementing only sigmoidal thresholding is presented which possesses a significantly improved output response (Fig. S4A).

Here, we make use of complex M, which is formed by combining an equal amount of $T2$ and $L1$. Subsequently, a small amount of $P1$ is added, and displaces $T2$, forming an equal amount of $D1$ and $T2$. Next, the sample with an unknown amount of $T1$ is added. $T1$ preferentially reacts with M because there are more toehold bases to initiate hybridization, and because the reaction is irreversible. Only when M is exhausted does $T1$ start to significantly react with $D1$. At this point, the $T1$ and $T2$ cooperatively hybridize to $D1$, releasing $P1$ which results in a fluorescence increase.

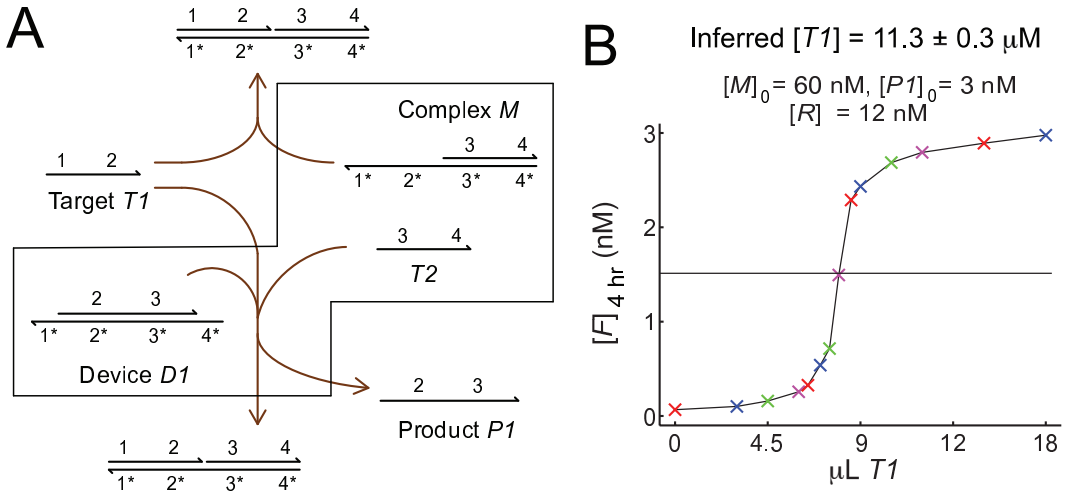

FIG. S4: Digital concentration comparison. **(A)** Standard complex M is pre-reacted with a small quantity of $P1$ to generate an equal small quantity of $D1$ and $T2$. Target $T1$ preferentially reacts with M, and reacts with $D1$ and $T2$ to release $P1$ only after $S2$ is exhausted. The box shows the species initially present before addition of sample containing $T1$. $P1$ subsequently reacts with reporter complex R to release fluorophore-labeled strand F (see Fig. 1B). **(B)** Fluorescence signal increases significantly if $T1$ is in excess of M. $[T1]$ was measured by UV absorbance to be 10 μM. Sigmoidal response curve allows precise quantitation. The fluorescence crosses the half-max threshold at 8.0 ± 0.2 μL T1, implying $T1$ concentration to be $\frac{1.5 \text{ mL} \cdot 60 \text{ nM}}{8.0 \pm 0.2 \ \mu\text{L}} = 11.3 \pm 0.3$ μM, assuming the $T2$ concentration is accurate.

Fig. S4B shows the fluorescence value 4 hours after the sample containing $T1$ is added. From this figure, the concentration of $T1$ is inferred to be 13% higher than that calculated from absorbance at 260 nm, assuming that the concentration of M is accurate.

S6. Characterizing oligonucleotide purity using denaturing PAGE

Other than fluorophore/quencher-labelled oligonucleotides, the DNA strands used did not undergo post-synthesis HPLC or PAGE purification. This was to demonstrate the error robustness of the cooperative hybridization mechanism, which functions despite some fraction of oligonucleotides containing deletions and 5' truncations. Here, denaturing PAGE is used to estimate the purity levels of the oligonucleotides.

Fig. S5A shows the denaturing PAGE that was used to analyze purities, while Fig. S5B through S5F show the intensity analysis of each lane. Strands $T1$, $T2$, $P1$, and $L1$ were not post-synthesis purified, while $F1$ possess the ROX fluorophore and was purified by HPLC.

In combination with the results shown in Fig. 6 in the main paper, these results attest to the robustness of the cooperative hybridization mechanism.

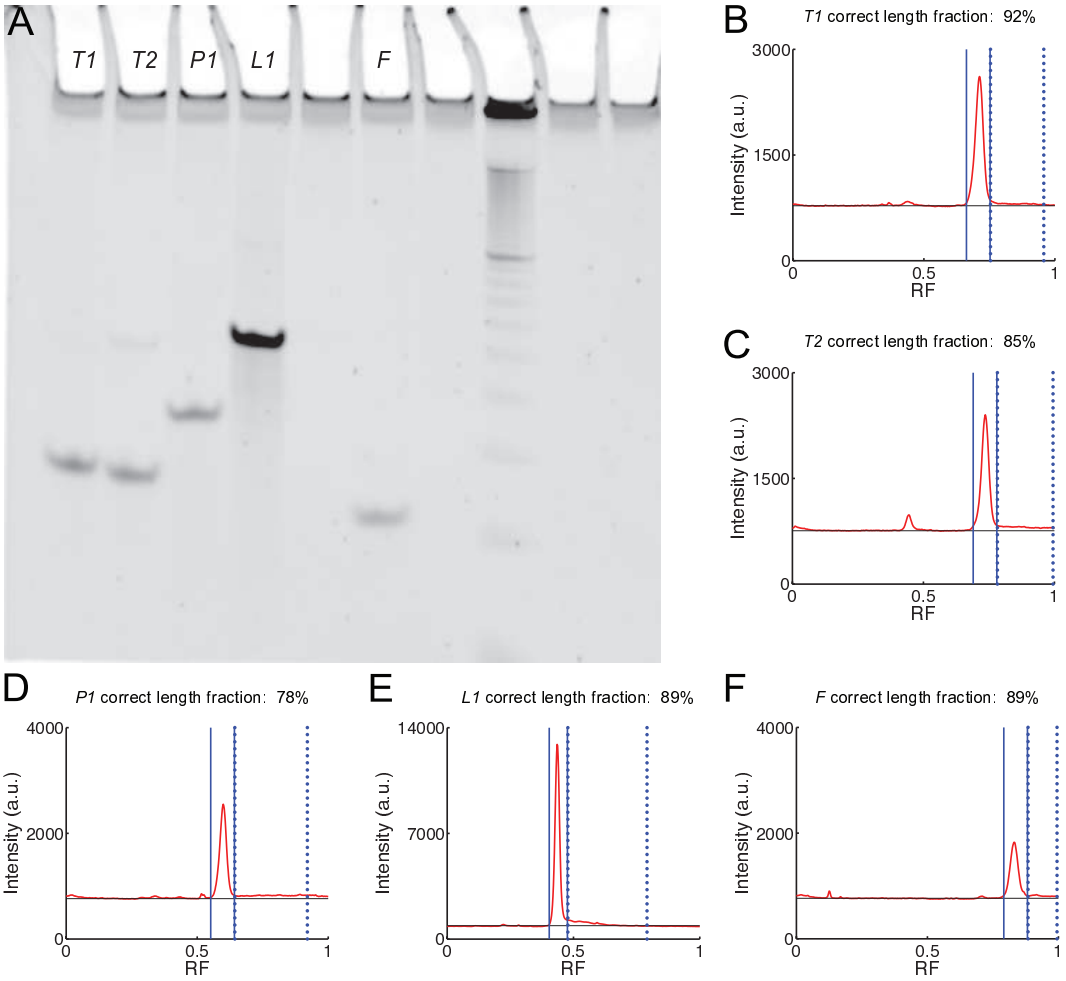

FIG. S5: Characterization of impurities present in the oligonucleotide samples. **(A)** Denaturing polyacrylamide gel electrophoresis (PAGE). **(B)-(F)** Lane analysis of each oligonucleotide species. The red trace shows the gel intensity against the relative front (RF). The black line shows the inferred background intensity, calculated from averaging the intensities between RF = 0.2 and 0.3. The area between the solid blue lines and above the background are assumed to be the correct length product, and the area between the dotted blue lines and above the background are assumed to be truncation products. The inferred fraction of correct length product is listed in each subfigure.

[1] SantaLucia, J. & Hicks, D. The thermodynamics of DNA structural motifs. *Annu. Rev. Biophys. Biomol. Struct.* **33,** 415-440 (2004).

[2] Gao, Y., Wolf, L. K.& Georgiadis, R. M. Secondary structure effects on DNA hybridization kinetics: a solution versus surface comparison. *Nucleic Acids Research* **34,** 3370-3377 (2006).

[3] Zhang, D. Y., Turberfield, A. J., Yurke, B. & Winfree, E. Engineering entropy-driven reactions and networks catalyzed by DNA. *Science* **318,** 1121-1125 (2007).

[4] Zhang, D. Y. & Winfree, E. Control of DNA Strand Displacement Kinetics Using Toehold Exchange. *J. Am. Chem. Soc.*

131, 17303-17314 (2009).

[5] Marras, S. A. E., Kramer, F. R. & Tyagi, S. Efficiencies of fluorescence resonance energy transfer and contact-mediated quenching in oligonucleotide probes. *Nuc. Acids Res.* **30,** e122 (2002).